A decision-support algorithm for post-earthquake water services recovery and its application to the 22 February 2011 M_w 6.2 Christchurch earthquake

Xavier Bellagamba,[a)] M.EERI, Brendon A. Bradley,[a)] M.EERI, Liam M. Wotherspoon,[b)] M.EERI, and Walter D. Lagrava[a)]

As the cost of lifeline disruption rises with the size and complexity of urban communities, increasing efforts are put into enhancing infrastructure resilience to natural disasters. Aiming to improve the understanding of water supply network seismic resilience, this paper examines in detail the initial performance and restoration of the water supply network following the 22 February 2011 M_w 6.2 Christchurch, New Zealand, earthquake. In addition, a method to optimize the recovery of such systems is developed in two phases: the prioritization of pipe inspection and the prioritization of pipe repairs. The results inferred from observed pipe repairs suggest that the recovery was carried out efficiently, however, applying the proposed methodology would have substantially improved the recovery of the system with a 30% reduction in the number of buildings deprived of water in the first two days. Assumptions and limitations of the modelling are also discussed and practical solutions given to apply this framework in real-time for post earthquake restoration.

INTRODUCTION

In increasingly connected and complex societies, infrastructure resilience and post-disaster recovery is receiving growing attention from public and private sectors, such as RESILENS (Hynes et al., 2016) from the European Union, Resilience to Nature's Challenges (Fraser, 2017) from the New Zealand Government and 100 Resilient Cities (Choi, 2017) from the Rockfeller Foundation. Acute stresses on infrastructure caused by extreme events, such as earthquakes, are recognized as a major factor in socio-economic disruption as observed by Rose et al. (1997); Tierney (1997); Dahlhamer et al. (1999); Miles and Chang (2006); Hallegatte (2008) and Love

[a)] University of Canterbury, Civil and natural resources engineering, 20 Kirkwood Ave, Upper Riccarton, Christchurch 8041, New Zealand

[b)] University of Auckland, Civil and environmental engineering, 20 Symonds St, Auckland 1010, New Zealand

(2011). In particular, disruptions in the water supply system can disable fire-fighting capabilities (Borden, 1997; Hughes et al., 2017); impede business and farming productivity, including tourism attractiveness (Rose et al., 1997; Stevenson et al., 2012, 2017); and alter the daily life of the resident population (McReynolds and Simmons, 1995 ; Chung et al., 1996, pp. 301 - 333 ; Hughes et al., 2017).

The aftermath of the 22 February 2011 M_w 6.2 Christchurch earthquake and its geotechnical consequences provide a stark illustration of the importance of resilient infrastructure (Bradley and Cubrinovski, 2011; Cubrinovski et al., 2011; Bradley et al., 2014; Bouziou et al., 2015). King et al. (2014) estimated that the costs of public infrastructure rebuild would be NZD 6 billion or 3% of the New Zealand GDP. Previously technical literature has extensively described the damage to the road, gas, water supply, sewerage and electricity networks, which were severely impacted by liquefaction and lateral spreading (Giovinazzi et al., 2011 ; Eidinger and Tang, 2012, pp. 152–171 ; Cubrinovski et al., 2014, pp. 10–45 ; O'Rourke et al., 2014). In particular, Giovinazzi et al. (2011) reported that approximately 50% of Christchurch was without water access on the day of the event and that it took a month to restore 95% of water supply services. By tracking the number of detected pipe failures over time, O'Rourke et al. (2014) estimated that the system was nominally restored after 53 days following the event.

In order to reduce the impact of lifeline disruption due to widespread system damage impacting functionality, several inspection and repair scheduling algorithms have been developed while optimizing the use of available resources. In particular, linear programming (LP) or mixed-integer linear programming (MILP) algorithms have proven relatively efficient to accelerate recovery processes of different lifeline systems, e.g. Yao and Min (1998) for electricity networks and Feng and Wang (2003) for the road networks. Fang and Sansavini (2017) proposed an MILP-based model that optimizes restoration of network connectivity, while mitigating future losses by rebuilding infrastructure in less vulnerable areas. While the latter approach suits strategic rather than urban infrastructure due to the high asset density and the already-existing redundancy in urban systems (e.g. high-voltage transmission power lines or continental gas pipelines versus power distribution grid, sewerage or water supply networks), solving any of these approaches can become prohibitly computationally expensive for large systems with current resources. In such cases, the optimum can alternatively be obtained by using metaheuristic techniques. For example, Xu et al. (2007) propose a genetic algorithm (GA)-based scheduling recovery process (inspection, damage assessment and restoration) for a collection of power stations that minimizes the number of people disconnected from the network over time. Power lines are not considered in the analysis and the problem's constraints are given by the number of repair teams. Bocchini et al. (2013) also use a GA-based algorithm to produce Pareto-set optimal solutions that maximize the connection between vertices of a road network composed of several bridges.

Few studies have focused on improving or measuring the resilience of water supply networks. Among these, Tabucchi et al. (2010) propose a restoration process for the Los Angeles City water supply network. It prioritizes the inspection of pipes based on their distance to the epicentre and repair based on the distance from the closest water source (e.g. wells or reservoirs). The primary objective of this method is to minimize the number of people disconnected during the recovery period. In their study, the water flow is simulated, however only main pipelines are considered, and the community is modelled as demand nodes. Klise et al. (2017) propose a software to analyse the resilience of water supply networks, which accounts for the water flow, the capacity to produce fresh water and the demand from the community. However, the suggested recovery strategy does not consider the inspection and damage assessment processes (i.e. it assumes all pipe failure locations and their severity are known).

Despite the efforts made to develop accurate recovery models for water supply systems, several problems remain. First, as emphasized by Zorn and Shamseldin (2016), interdependencies between systems can play a crucial role in their respective functionality. This is particularly true for water supply systems, which are highly reliant on the functionality of the electric power network. Second, the detection of pipe failure can mobilize a non-negligible portion of the available human resources and take several weeks as noted by Hughes et al. (2017) in the context of the 14 November 2016 M_w 7.8 Kaikoura earthquake. Third, as new pipe failures are detected, repair priorities might evolve. Hence, a periodic re-assessment of the repair priorities is necessary to ensure the implementation of the optimal solution.

In this paper, the historical recovery of the Christchurch water supply following the 22 February 2011 event is inferred from reported pipe failures and a GA-based optimization method for post-earthquake recovery dedicated to water supply systems is proposed. The recovery is expressed utilizing city-scale metrics such as the number of impacted buildings, the population or the building utility (see Table 1) and explicitly accounts for the dependency on the functionality of the electric power network. The proposed optimization method operates on a periodic basis and minimizes a weighted combination of the population, the utility of buildings and the number of buildings disconnected from the water supply system. Finally, both the historical and optimized recoveries are compared.

INFERRED RECOVERY OF THE WATER SUPPLY NETWORK FOLLOWING THE 22 FEBRUARY 2011 M_W 6.2 CHRISTCHURCH EARTHQUAKE

This section briefly describes the datasets used in the historical analysis, the assumptions and the results of the inferred co-seismic performance of the water supply network. The phrase '*inferred*' is used to indicate that quantitative metrics to describe network-level recovery were not directly catalogued, but are reconstructed through more granular, historical records combined with an understanding of the network topology and interviews with water supply network personnel. In addition, the inferred co-seismic performance is compared to a prediction considering the same assumptions, where pipe failures are generated through a Monte-Carlo simulation scheme. The historical recovery is then derived from reported pipe repairs and discussed with respect to the community.

WATER SUPPLY NETWORK AND COMMUNITY DATASETS

The Christchurch water supply network is composed of 3,246 kilometres of pipelines, out of which 1,612 kilometres are trunk main or main pipelines and 1,634 kilometres are submain or crossover pipelines. Cubrinovski et al. (2014, pp. 3–9) provide an accurate description of the pipe network in terms of topology, material composition and technology. The analysed network is supplied by 92 pump stations out of which 23 have a diesel generator allowing them to operate during long power outages. Most pump stations are located nearby a water supply source (bored wells or tanks). A few exceptions are located in low density residential suburbs in the Port Hills area.

The Christchurch community is described by three different datasets: (1) the land usage that provides the category of buildings (business, medical, school, residential, rural or critical) (M. Hughes, pers. comm.); (2) the building footprints that gives the location and geometry of each building (M. Hughes, pers. comm.); and (3) the census that provides an estimate of the population over meshblocks, areas delineated by the New Zealand authorities for this specific purpose (Statistics New Zealand, 2013a). To reduce the computational burden and avoid misassignment of population to buildings, building footprints of less than 20 square meters were removed, while building footprints more than 200 meters from a submain pipe were considered off-grid and also removed. The final building footprint dataset enclosing the usage informa-

Table 1. Christchurch City Council utility values (Irmana Garcia Sampedro, pers. comm.)

Utility value	Description	Categories
1	Very low	Rural ; Residential
2	Low	Commercial ; Industrial
3	Medium	School ; Childcare ; High water usage
4	High	Hospital without emergency facilities ; Rest home ; Emergency services ; Correction department facility ; General practitioner office
5	Very high	Lifeline facility ; Civil defence welfare center ; Hospital with emergency facilities

tion contains 209,442 buildings, of which 8,008 are business buildings, 2,239 school, childcare or university buildings, 355 hospitals or medical buildings and 55 critical buildings, with the remainder being essentially composed of residential, rural, cultural and recreational buildings. Based on the usage category, the Christchurch City Council assigns utility of buildings values to buildings as presented in Table 1. These values represent the importance of the building for the functioning of the community. As the acquired building dataset does not possess all presented categories, the distribution of utility value is slightly simplified: the label *High water user* is ignored, there is no utility value equal to 4 and a value of 5 is given to all medical buildings (i.e. to *hospital without emergency facilities, rest homes and hospital with emergency facilities*). To assign population to buildings, it is assumed that people can only occupy *Residential* and *Rural* buildings. As the 2011 population census was not carried out due to the 2010-2011 Canterbury earthquake sequence (Statistics New Zealand, 2013b), the population is estimated by a linear extrapolation from the two previous censuses realized in 2001 and 2006 by the Statistics New Zealand (2013a). The estimated population in 2011 in the considered buildings is approximately 351,500 people. The population was then assigned to each *Residential* and *Rural* building depending on the density of population over the inhabitable area of the meshblocks and the building footprint size. Figure 1 shows the different usage of the building footprints and the Christchurch water supply network.

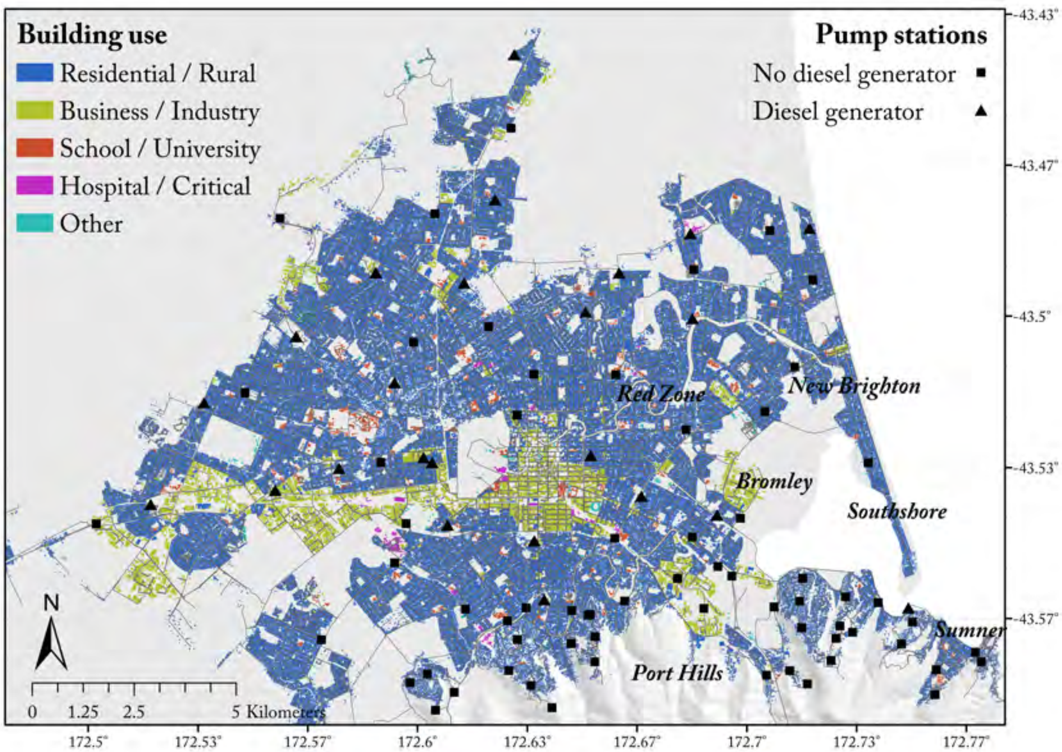

Figure 1. Map of the Christchurch building stock annotated according to building use, water supply pipe network and pump stations

ESTIMATED INITIAL PERFORMANCE AND ITS MODELLING

The 22 February 2011 M_w 6.2 Christchurch earthquake caused 3,039 pipe failures (Eidinger and Tang, 2012, p. 159), mostly due to severe liquefaction and lateral spreading. Cubrinovski et al. (2014, p. 19) discussed their geospatial distribution and O'Rourke et al. (2014) provide the observed daily repair rate and inferred the '*effective*' completion of the earthquake-related repairs on the 15th of April 2011, 53 days after the earthquake. Immediately after the earthquake, large portions of the city were also in areas with power outages (L. Dueñas-Osorio, pers. comm. ; Fenwick et al., 2011), disabling the majority of the pump stations. Access to power was the most important factor for the network in order to operate pump stations (K. Snyder-Bishop, pers. comm.).

Two neighbouring pump stations located in the Port Hills (South-East of the city; Figure 1) suffered from critical failures (one from cliff collapse, see Dellow et al. (2011) for more details, and the other from extensive structural damage) and have not been brought back to service (K. Snyder-Bishop, pers. comm.). To estimate the initial impact of pipe failures and disabled pump stations, several assumptions have been made. First, water flow is not explicitly considered for computational reasons as detailed in a subsequent section (i.e. the proposed work is based solely on pipe connectivity). However, given the relatively uniform geospatial distribution of the pump stations across the city, it is believed that this assumption has only a second order effect. Furthermore, the type and severity of pipe damage has not been adequately documented, such that individual pipe functionality cannot be inferred. Hence, this analysis monitors the *water delivery* as defined in Davis (2014). Second, a pipe is assumed to have lost its connection if at least one failure has occurred on all its potential routes from any source or on itself (as presented in Equation 1 below). Third, pump stations equipped with a diesel generator have been brought back to service within the first 24 hours of the earthquake as road access was not a major problem in Christchurch (Eidinger and Tang, 2012, pp. 248–265). Hence, diesel-powered pump stations were considered out of service only on the day of the event itself. Fourth, despite minor relocation of population and businesses (Stevenson et al., 2011; Chang et al., 2014), buildings are considered to require reconnection to the water supply (i.e. they are all considered as a demand node for water resources, irrespective of what their damage state was). Note that this assumption is consistent with the fact that government-provided temporary housing was unused and quickly closed down (Giovinazzi et al., 2012). Fifth, buildings are assumed to be connected to their closest submain and private connections from the submains to the buildings are not considered. Finally, as long as one undamaged pipeline route exists from a building to a pump station, the former is considered connected to the latter as expressed in Equation 1.

$$\begin{cases} \text{Connected,} & \text{if} \quad \min_{1 \leq j \leq M_i} N_{fail,i,j} = 0 \\ \text{Disconnected,} & \text{otherwise} \end{cases} \tag{1}$$

where M_i is the number of potential routes from any source to building i and $N_{fail,i,j}$ is the number of pipe failures on existing route j of building i. Note that this equation is also valid to assess pipe connectivity status.

As subsequently discussed, to optimize the recovery process, pipe damage and building connectivity predictions are necessary. Damage prediction is evaluated for each individual pipe and uses the pipe fragility functions developed from Christchurch damage data by Bellagamba et al. (Accepted). These functions require, in addition to the pipe characteristics (length, material and diameter), the estimated peak ground velocity (PGV) and the liquefaction susceptibility of the soil expressed as its cyclic resistance ratio (CRR) at pipe installation depth. The PGV is probabilistically generated as a spatially correlated random field using the median and standard deviation of the PGV estimated by Bradley (2014) and the spatial correlation coefficient proposed by Jayaram and Baker (2009). The CRR is inferred from the liquefaction resistance index map compiled by Cubrinovski et al. (2014, pp. 13–15) as proposed by Bellagamba et al. (Accepted). Building connectivity is assessed following the procedure used to infer the inferred initial network performance. To achieve stable results, 2000 realizations from the Monte-Carlo scheme were executed and sufficient convergence was attained. Either inferred or predicted, the performance and recovery of the water supply network are expressed by means of community-oriented metrics at two levels of granularity - global and specialized. The three global metrics measure the population, utility of buildings and number of buildings (all types) deprived of water. The specialized metrics quantify the business, medical (including hospitals and rest homes), school (including universities and childcare) and critical buildings deprived of water.

Figure 2(a) presents the results of the inferred co-seismic performance, whereas Figure 2(b) shows the results of the prediction. The difference between the reported (50% of the dwellings without water access immediately after the earthquake reported by Giovinazzi et al., 2011) and inferred number of buildings deprived of water indicates that not considering the water flow during a generalized power outage leads to a significant underestimate of the initial impact. However, because the power outage only lasted one day for most of the city (L. Dueñas-Osorio, pers. comm. ; Fenwick et al., 2011), it is expected that the map presented in Figure 2(a) approximately reflects the real state of the water outage by the end of day 1 following the earthquake.

The eastern suburbs of Christchurch (New Brighton, Southshore and Sumner; indicated in Figure 1) as well as the most severely liquefied areas (along the Avon River, also known as the *Red zone*; Figure 1) are the areas where most of the simulated outages take place. The former are indeed likely to suffer from an outage as they are topologically easily isolated and the latter are the most vulnerable to suffer from large permanent ground deformations (Cubrinovski et al., 2011), leading to extensive pipe damage. Some areas in the Port Hills (South of the city; Figure 1) might have been more impacted than what is shown in Figure 2(a) due to the pressure loss caused by altitude changes, which was not explicitly modelled as previously noted. Figure 2(b) presents the prediction results and illustrates important similarities with the inferred co-seismic initial impact: a significant portion of the buildings likely to lose their connection to the water supply network (i.e. probability of water outage $\geq$50%) are, according to the inferred co-seismic performance, disconnected from the water supply network. It must be noted that building connectivity is relatively well predicted, whereas pipe damage remain inaccurate. Further details such as the receiver operation characteristics (Fawcett, 2006) for both pipe dam-

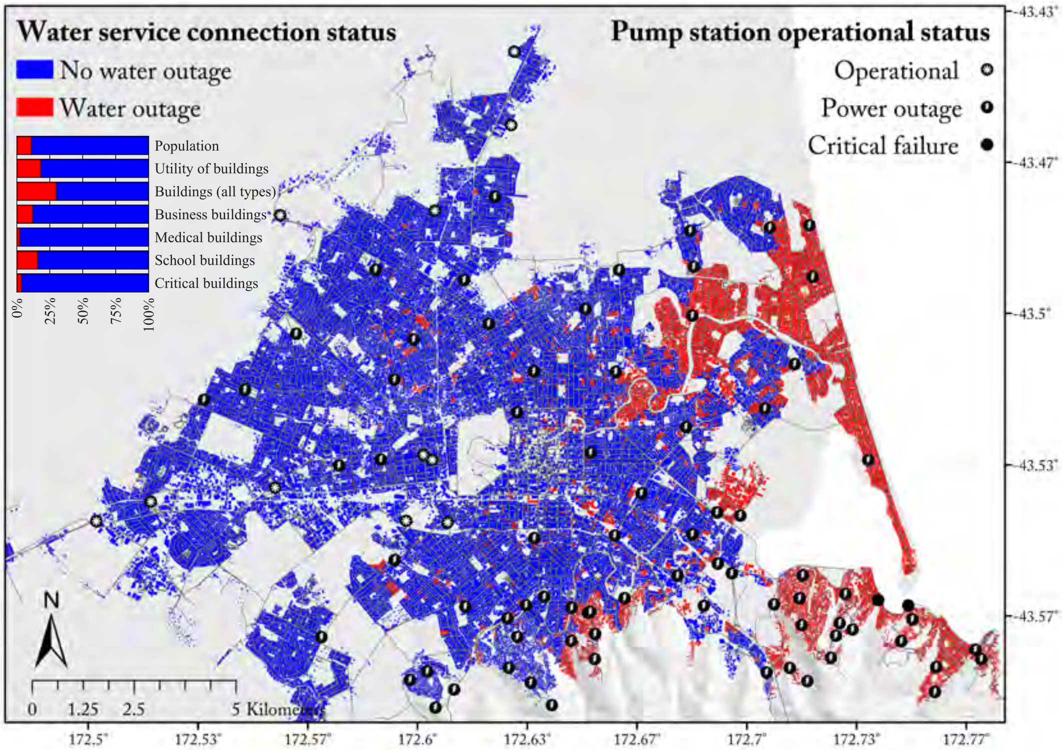

(a)

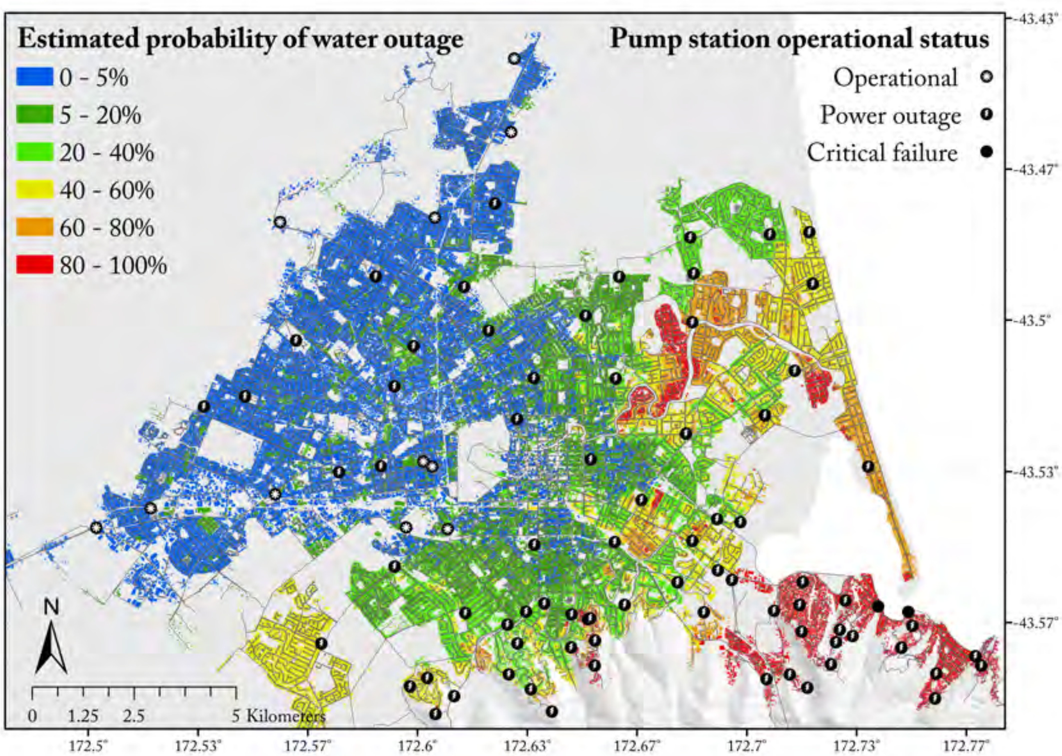

(b)

Figure 2. Water supply network performance following the 22 February 2011 M_w 6.2 Christchurch earthquake: (a) Map of the inferred co-seismic water outage and histogram indicating the portion of each considered metric suffering from water outages ; (b) Map of predicted initial water outage (probability of water outage)

age and building connectivity, and the differences between the inferred and predicted analyzed metrics can be found in the electronic supplement in Figures A.1 and A.2, respectively.

INFERRED WATER SERVICE RECOVERY

Following the Christchurch earthquake, the recovery started quickly. Most suburbs recovered access to electricity on the day after the earthquake (L. Dueñas-Osorio, pers. comm. ; Fenwick et al., 2011). Pump stations were restored once electricity access was restored or when their diesel generator was turned on. Despite the existence of damage, and excluding the two suffering from critical failures, all pump stations were able to deliver some outflow (K. Snyder-Bishop, pers. comm.). Pipe failure detection was realized following a two-step iterative process. First, pump stations were required to deliver their maximal outflow and then, repair teams were in charge of detecting any major leakage from abnormal traces of water on the surface. This process started near the pump stations and, as repairs were executed, inspections were moved away from their original start point. A repair priority varying from 1-10 days was assigned to every detected pipe failure. It is worthy to note that only the dates of detections are known, not the actual dates of repairs completed as described in the pipe failure dataset. A peak of 300 repair teams has been noted by Eidinger and Tang (2012, p. 159). According to the Christchurch City Council estimations reported by Giovinazzi et al. (2011), the system had recovered approximately 95% of its serviceability a month following the earthquake. Eidinger and Tang (2012, p. 159) inferred the full recovery of the system 40 days after the earthquake (on the 5th of April), whereas O'Rourke et al. (2014) made a corresponding estimate of 53 days (on the 18th of April). Note finally that the results presented here do not consider the temporary bypasses and pumps as well as isolation capabilities of the water supply network that may have been put in place and use during the recovery to reduce the global disruption.

As the pipe repair dates are unknown, 100 realizations of the historical recovery are simulated. The delay between the discovery of a pipe failure and its repair is assumed following a discrete uniform distribution as shown in Equation 2.

$$\text{Delay}_i \sim \mathcal{U}(1, \text{priority}_i) \tag{2}$$

where $\sim \mathcal{U}$ denotes that $Delay_i$ is sampled following a uniform distribution and $priority_i$ is the assigned priority of pipe failure i. The delays are assumed independent from each other (i.e. no correlation between delays is applied). Figure 3 presents the map of the simulated average water outage time. Similarly to the initial performance estimation, because the model does not consider water flow, the outage in the central and eastern suburbs of the city are underestimated by 1 day. It is easy to observe that the most isolated parts of the city (New Brighton, Southshore and Sumner; 1) are the latest to recover water access. In these areas, electricity was restored relatively late and therefore pump station functionality could not be restored in a timely manner. The *Red zone* and its neighbourhood also required a long restoration period as the system was heavily damaged due to severe liquefaction and lateral spreading.

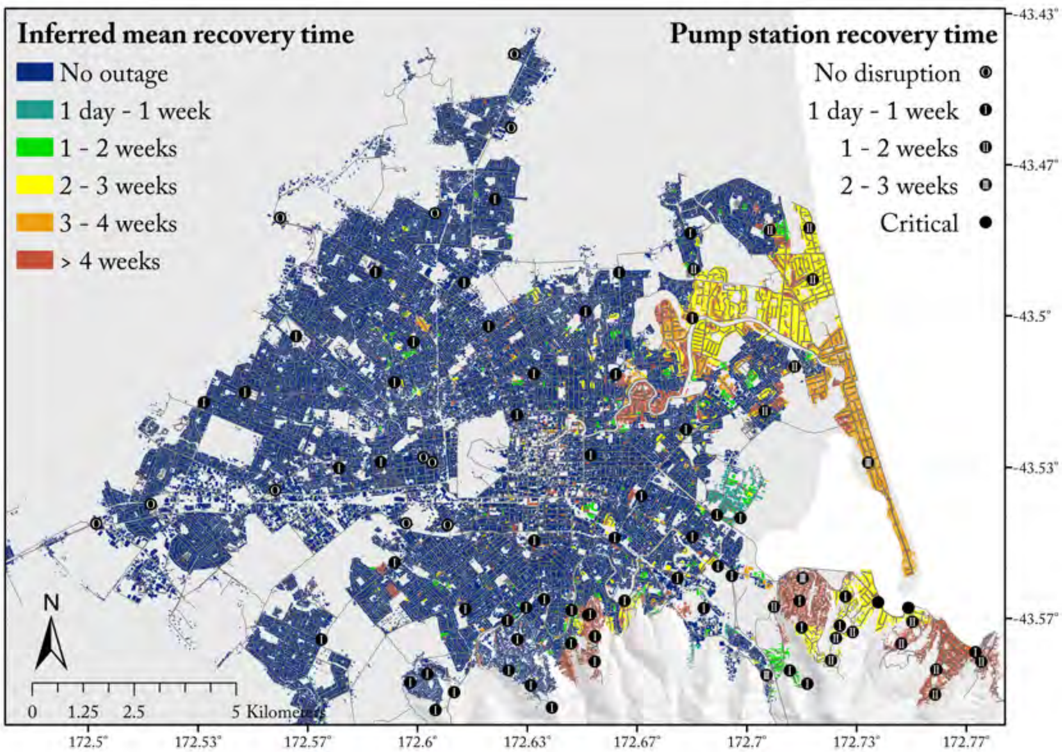

Figure 3. Map of mean time for reconnection to water supply network following the historical recovery process inferred from the dates of reported pipe repairs following the 22 February 2011 M_w 6.2 Christchurch earthquake

Figure 4 shows the recovery curves over time and resilience of all selected metrics as well as the number of pump stations remaining non-operational. The resilience R is estimated as proposed by Cimellaro et al. (2010, Eq. 1) and reproduced in Equation 3.

$$R = \int_{t_{0E}}^{t_{0E}+T_{LC}} Q(t)/T_{LC} \mathrm{d}t \tag{3}$$

where t_{0E} is the occurrence time of the event, T_{LC} is the control period of the system set to the entire recovery time and $Q(t)$ is the functionality of the system in percent depending on the time. In the considered case, the control period is therefore set to 63 days (the recovery period), dt is set to one day, and $Q(t)$ is the inferred performance of each selected metrics. Based on the proposed model, it is worth noting that the pump stations apparently played a second order role in the recovery of the water supply access. However, the reported disruption levels by Giovinazzi et al. (2011) seem to be more strongly correlated with the restoration of the pump stations' operability. This supposes that, as long as a significant portion of the pump stations are non-operational, a connectivity approach might not be sufficient to accurately assess the systemic disruption. Nevertheless, this approach appears to be accurate once the majority of the pump stations are brought back to service (around the 7$^{\text{th}}$ day of the recovery). Despite a lower initial estimate, the model seems to corroborate the observations made in previous studies: the 7% disruption (*Buildings (all types)* metric) left after 30 days of recovery is consistent with the 95% of service restoration reported by Giovinazzi et al. (2011), and most of the buildings and population in the simulations had recovered their water access after the 6 weeks proposed by Eidinger and Tang (2012, p. 159) as the end of the post-earthquake repair period. The inflexion point (where the repairs start to have a significant effect on the attenuation of the disruption) occurs around the 15$^{\text{th}}$ day, when the northern parts of New Brighton were serviced again (north-eastern yellow areas in Figure 3).

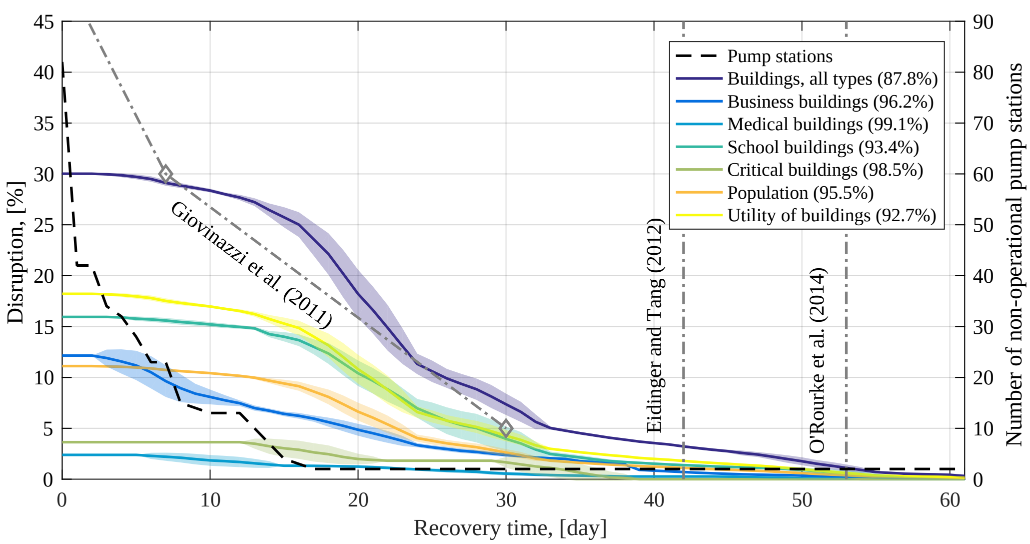

Figure 4. Mean water access recovery curves of the selected metrics following the 22 February 2011 M_w 6.2 Christchurch earthquake (shaded areas represent the first standard deviation boundaries of each metric) ; estimated completion of the repair work by Eidinger and Tang (2012) and O'Rourke et al. (2014) ; and interpolation between the levels of disruption (indicated by diamonds) reported by Giovinazzi et al. (2011). Numbers between brackets indicate the resilience of each metric estimated with Cimellaro et al. (2010, eq. 1).

As observable in Figure 4, the shape of the presented recovery curves follows a cosineshape, which is attributed to a "*not well prepared community*" by Cimellaro et al. (2010). This classification should be further interrogated in relation to a number of factors. First, at the beginning of the repair period (about one day), the real recovery curve may be closer to the disruption level interpolation reported by Giovinazzi et al. (2011), which follows an exponential function and can therefore be related to a "*well prepared community*". Second, as the water supply system possesses a strong dependency to the power grid, the water supply system has to "wait" for the restoration of the electric power network, or has to operate on alternative power sources (e.g. diesel-powered backup systems). Third, the damage detection of underground systems requires more resources than systems that are located at the surface, slowing down the actual repair process. Finally, as aforementioned, the potentially positive effects of temporary measures have not been taken into account, reducing the measured resilience of the system.

PROPOSED RECOVERY OPTIMIZATION METHODOLOGY BASED ON A GENETIC ALGORITHM

In the development of their framework, Bruneau et al. (2003) characterize the seismic resilience of a system with its robustness, redundancy, rapidity and resourcefulness. Therefore, based on the observed system robustness and existing redundancies, the use of its resources and its rapidity to react can be optimized. As observed during the water supply restoration in Christchurch, the detection of the pipe failures can take a non-negligible time, leading to potential changes in the optimal repair priorities. Hence, these repair priorities have to be periodically re-evaluated in order to improve the resilience of the system by maximizing the effect of the repairs on its serviceability. The constraints of the problem are the periodic capacity to inspect and repair pipes (i.e. the maximum inspectable pipe length and the maximum number of executable pipe repairs, respectively). In this section, an inspection priority ranking approach is described, and the proposed GA-optimized repair process explained.

INSPECTION PRIORITY LIST

Based on predicted damage and serviceability results, an inspection priority list is established. This list ranks the pipes based on the inverse of their probability of survival, and on their probability of connection survival due to their own failure, as proposed in Equation 4. The probabilities of pipe disconnection are estimated considering all working or repairable pump stations (i.e. only excluding pump stations suffering from critical failure). Hence, inspections prioritize pipes with high probability of failure and low probability of disconnection (closer to a working or repairable pump station).

$$\text{Score}_i = \frac{1 - P_{Disc,i} + P_{f,i}}{\left(1 - P_{f,i}\right)^2 + \epsilon} \tag{4}$$

where $P_{f,i}$ is the failure probability of pipe i from pipe fragility analysis, and $P_{Disc,i}$ the disconnection probability of pipe i from network connectivity analysis. A small value ϵ (0.00001) is added to the denominator to avoid division by 0. $P_{Disc,i}$ is computed from Equation 5.

$$P_{Disc,i} = \min_{1 \le j \le N_i} P_{Disc,i,j} \tag{5}$$

$$\text{with} \qquad P_{Disc,i,j} = 1 - \prod_{k=1}^{m_j} \left(1 - P_{f,k}\right) \tag{6}$$

where N_i is the number of potential routes from any water source to pipe i, and $P_{Disc,i,j}$ is the disconnection probability of route j composed of m_j pipes. The inspection priority list is compiled only once at the beginning and remains unchanged for the entire recovery process for computational reasons. This method is limited by the inability of some of the pump stations to operate at the creation of the list, as they are, for example, not able to access electric power. However, as the first failed pipe on a particular route receives the highest priority, and although it simplifies the inspection process as it has been carried out, the list is believed to optimize it in a relatively realistic fashion.

FORMULATION OF THE REPAIR OPTIMIZATION LINEAR PROGRAM

As mentioned earlier, the recovery process of a spatially-distributed infrastructure system can be expressed as an MILP, whose objective function minimizes the loss of serviceability. Here, the repair optimization takes into account the two parallel processes occurring during the recovery: (1) inspection of the network, and (2) individual pipe repairs. During each repair period, uninspected pipes having the highest inspection score are inspected such that the entire inspection capacity is used. Newly discovered pipe failures are added to the potential repair list at the end of the repair period. In parallel, the serviceability at each repair period is optimized with an MILP that minimizes a weighted combination of the population, the number of buildings and the utility of buildings deprived of water by prioritizing pipe repairs constrained by the maximum repair capacity. In other words, the objective of the program is the minimization of a linear combination of variables representing the outage impact, decision variables are the detected and unrepaired pipe failures, and the constraint is given in terms of time-dependent repair capacity. Note that the optimal solution of an iteration is agnostic to the optimal solution of the previous one (i.e. the algorithm gives the optimal tactical solution but does not follow a global strategy over time). Equations 7 to 11 mathematically set the considered MILP.

$$\min \qquad \Xi = \sum_{i=1}^{N} \left[Q_i \cdot \min \left(1; \min_{1 \le j \le M_i} N_{fail,i,j,t} \left(\Upsilon_{R,t}, \Upsilon_{I,t} \right) \right) \right] \tag{7}$$

$$\text{subject to} \qquad \|\Upsilon_{R,t}\|_1 \le C_{R,t} \tag{8}$$

$$\|\Upsilon_{I,t}\|_1 \le C_{I,t} \tag{9}$$

$$\text{with} \qquad Q_i = \sum_{k=1}^{L=3} w_k q_{i,k} \tag{10}$$

$$\text{and} \qquad \sum_{k=1}^{3} w_k = 1 \tag{11}$$

where N is the number of buildings in the dataset, Q_i is the quantity of the objective metric of building i, M_i is the number of potential routes from any source to building i, $N_{fail,i,j,t}$ is the number of pipe failures on existing route j of building i computed at the end of period t. $N_{fail,i,j,t}$ depends on decision variables $\Upsilon_{R,t}$ and $\Upsilon_{I,t}$, the allocation of the repair and inspection capacities over period t, respectively. Their respective Manhattan norm $\|\Upsilon_{R,t}\|_1$ and $\|\Upsilon_{I,t}\|_1$ represents the utilized repair and inspection resources over period t. $C_{R,t}$ and $C_{I,t}$ are scalars expressing the maximum repair and inspection capacities over period t, respectively. Inspection and repair capacities are given in terms of pipe length and pipe failures, respectively. In a real case, those values will depend on the available human and financial resources and construction material and require careful assessment as discussed in Section 4.3. The quantity Q_i is computed as the sum of products between the objective function weights w_k and the three considered quantities $q_{i,k}$. For this work, three different quantities are considered to be optimized: (1) the population; (2) the utility of buildings; and (3) the number of buildings (always equal to 1 for a single building). The weights w_k must be set with respect to the recovery manager's objectives. Weighting based on the maximum number of buildings alone may be appropriate for rural areas where authority-owned buildings may not be able to shelter and provide services for a large number of people. Hence accelerating the service recovery of a large number of buildings (houses and farms) can be seen as critical. The combination of two or more quantities may be more suitable to urban areas, as recovery officers may want to restore services for productive capacities and critical facilities more quickly than in rural areas. The density being generally higher in urban than rural areas, targeting the population and utility would have a greater positive effect on the population and economy than targeting the number of buildings.

IMPLEMENTATION OF THE GENETIC ALGORITHM

The periodic allocation of repair resources can be encoded as a binary vector composed of 0 for *do nothing* and 1 for *repair* as proposed by (Fang and Sansavini, 2017, Eq. 10). Following the same reasoning, the periodic allocation of inspection resources is encoded as 0 for *do nothing* and the length of pipe occupying a given position in the vector for *inspect*. The size of both vectors represents the number of pipes in the system and the number of non-repaired pipe failures for the inspection and repair vectors, respectively. However, as the inspection ranking list is immutable, the allocation of the inspection capacity is predetermined for each period. The dimension of the problem (i.e. the number of decision variables it contains) is then determined by the number of unrepaired pipe failures. The search space of the MILP therefore becomes the set of all potential repair permutations. The permutation number can be computed as a binomial coefficient with the number of non-repaired pipe failures and the repair capacity as coefficients. As the problem can rapidly become very large and have multiple local minima, brute force approaches or convergence algorithms would be inefficient and lead to suboptimal solutions. Given the encoding of the problem, its size and the potentially non-convex search space, a genetic algorithm (GA) was implemented, which is recognized as an efficient method to solve such problems (Mitchell, 1998, pp.116 –117). GA does not always deliver the optimal solution but yields a '*good*' solution at lesser computational expense than other techniques. However, GA requires a maximization problem. Hence, the objective function presented in Equation 7 is transformed into a maximization problem presented in Equation 12, whereas the constraints do not change.

$$\Xi = \sum_{i=1}^{N} \left[Q_i \cdot \left(1 - \min \left(1; \min_{1 \leq j \leq M_i} N_{fail,i,j,t} \left(\Upsilon_{R,t}, \Upsilon_{I,t} \right) \right) \right) \right] \tag{12}$$

In the GA context, a set of potential solutions of the problem is called a *population*. Individuals of this population are called *chromosomes* and their characteristics, *alleles*. Here, chromosomes are the daily repair solutions that satisfies the constraints (i.e. they are part of the search space) and alleles represent each detected, but unrepaired, pipe failure. An allele encodes a *trait*, the value of the allele (in our case, *repair* or *do nothing*). A *locus* represents the position of a particular allele on a chromosome. Hence a particular locus represents the position of a particular pipe failure in the database. The ability of a chromosome to survive or reproduce is given by its *fitness*, computed as the result of the objective function in Equation 12.

To converge toward a fitter population, chromosomes *mate* with each other in pairs over steps called *generations*. The mating process consists of three distinct operations: *selection* (which chromosomes mate), *crossover* (which alleles are exchanged between mating chromosomes) and *mutation* (which alleles are randomly modified). The mating process between two chromosomes creates two *offspring*. More information about GAs and their implementation can be found in Mitchell (1998) and Haupt and Haupt (1998).

In this study, the selection of chromosomes is realized via a binomial tournament and elitism. The former operator randomly picks two chromosomes from the current population and select the fittest ones for reproduction, allowing small fitness chromosomes to mate and slowing down the convergence rate of the algorithm, whereas the latter retains the best N_{elite} chromosomes of each generation for the next one without altering them. Parametrized uniform crossover is chosen as the crossover operator and locus swap as the mutation operator. The parametrized uniform crossover operator assigns the same probability of exchanging traits for all loci from both mating chromosomes. Once the offspring are created, the mutation operator decides if the encoded trait of two randomly chosen loci of the same chromosome are exchanged. Once the new generation is ready, it replaces the old one and the whole process is repeated a determined number of times or until a local optimum has been found (i.e. the standard deviation of the population fitness is equal to 0).

CASE STUDY: WATER SUPPLY NETWORK RECOVERY FOLLOWING THE 22 FEBRUARY 2011 M_W 6.2 CHRISTCHURCH EARTHQUAKE

To test the efficiency of the proposed GA optimization the Christchurch water supply network recovery following the 22 February 2011 M_w 6.2 earthquake was considered. The number and location of the pipe failures, the operational status and restoration time of pump stations are identical to that presented in Section 2. In the paragraphs that follow, first, the assumptions and parameters required to carry out the GA-based process are given. The optimized recovery curves and map are then presented and discussed in relation to the resilience metrics. Finally, the procedure for real-time application of this method is given.

OPTIMIZATION PARAMETERS

In order to account for missing information (e.g. the number of repair teams over the recovery period), several assumptions were made. Justifications for the parameter choices and assumptions are given in the next paragraph. The repair period is fixed to one day (i.e. repair priority assignment and system functionality are evaluated every day). The daily repair capacity is set to 50, the daily inspection capacity is set to 55 kilometres, the objective function weights are set to 0.5, 0.0 and 0.5 for the population, the number of buildings and the utility of buildings, respectively. The genetic algorithm is parametrized with a number of elite chromosomes of 2, a crossover rate of 75% and a mutation rate of 20%. Each generation contains 10 times the number of decision variables or a maximum of 1,000 chromosomes and the maximum number of fitness evaluations (the computational budget) is set to 5,000 per daily solution.

The daily repair and inspection rates represent the average observed repair rate following the Christchurch earthquake, due to the lack of the specific data enabling a time-varying rate to be reasonably assigned. This simple assumption allows all pipe failures to be discovered and repaired over the observed recovery period of 62 days (i.e. that the recovery period following the optimization process is not excessively longer or shorter than the observed one). However, as noted by (Eidinger and Tang, 2012, p. 159), these quantities have largely varied over time during the Christchurch recovery as resources were pulled out of neighbouring regions to participate to the restoration effort. The restoration capacity in a real case is treated in Section 4.3. The assigned weights give the same importance to the population and the utility of buildings, excluding de facto non-critical and non-inhabited buildings from the optimization process (e.g. sport and cultural facilities). This choice is consistent with previous observations made on the weighting choice presented in Section 3.2. However, given the relatively low population density of Christchurch (most of the buildings are family houses), results are not expected to be significantly different with another weighting. The GA-related parameters are chosen such that a relatively high diversity of chromosomes is held over generations by enforcing most of the genes to be exchanged between mating solutions and frequent mutation. The number of different solutions per optimization problem is set according to the recommendations of Storn (1996) and Mallipeddi and Suganthan (2008) for low dimensionality problems. In addition to the computational burden a large chromosome population imposes, it is seen as an obstacle to convergence in evolutionary algorithms (Mallipeddi and Suganthan, 2008 and Chen et al., 2015). Hence, fixing its upper bound should also improves its convergence. Fixing the computational budget for each periodic solution, the number of generations inversely varies with the population size such that the total number of chromosomes does not exceed 5,000 fitness evaluations (i.e. the minimum number of generation is five). Hence, the algorithm can create up to a maximum of ten generations, when the population size does not exceed 500 chromosomes.

OPTIMIZED RECOVERY

Figure 5 presents the optimized water service restoration time given the observed pipe failures and aforementioned assumptions. The pump station restoration time is identical to that presented in Figure 3. The application of the proposed methodology leads to noteworthy improvements when compared with the inferred recovery in Figure 3. First, North New Brighton (location indicated in Figure 1) recovers faster than was inferred from historical repairs in Figure 3. Moreover, most of the Port Hills region regains access to the water supply system more quickly. However, the *Red Zone*, Bromley, Southshore and the rest of New Brighton suffer from longer water outages. This is explained by the difficulty that the inspection algorithm has in efficiently targeting pipes that have actually failed as subsequently discussed.

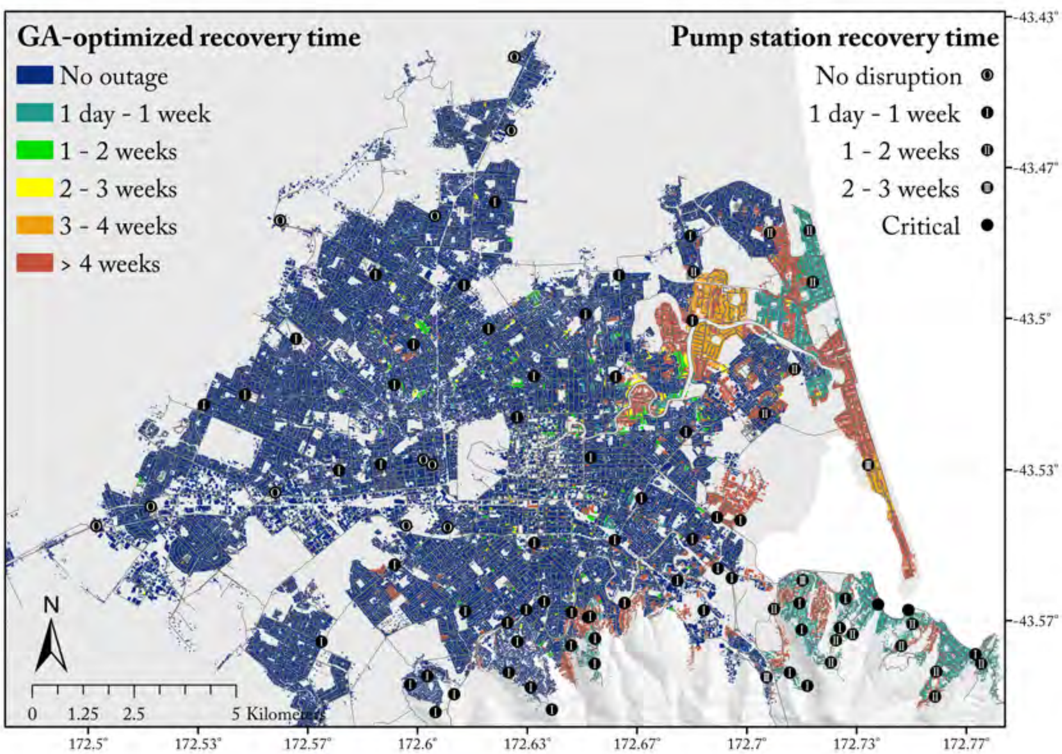

Figure 5. Map of time for reconnection to water supply network after the 2011 February M_w 6.2 Christchurch earthquake following the GA-optimized process

Figure 6 illustrates the optimized recovery curves and comparison to the inferred recovery curves. Most of the analysed metrics exhibit a steeper slope at the beginning of the recovery. This highlights the significant gains possible by optimization with an emphasis on pipes with high failure probability, low disconnection probability, and those servicing large community areas. A relatively steep slope is also observed after 21 days of recovery and corresponds to the power restoration of the New Brighton pump station and some repairs carried out in the *Red Zone*. However, the rate of improvements tend to be nullified over time. As the failure of individual pipelines is poorly predicted as noted in Figure A.1 (a), the inspection schedule (the order in which pipes are inspected) fails to efficiently prioritize actually damaged pipes using Equation 4. In other words, as pipe inspection becomes less accurate, the number of interesting repair options tends to diminish over time. This issue could be mitigated by assessing the probability of failure with multiple or other fragility functions based on more advanced statistical methods (e.g. Bagriacik et al., 2018).

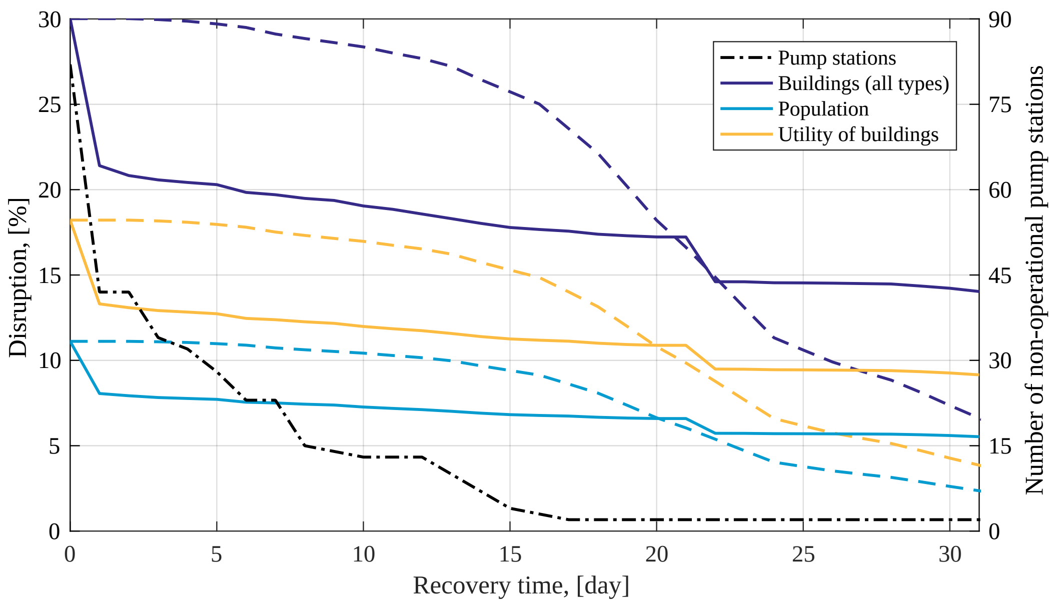

Figure 6. Pump station restoration curve and water access recovery curves of the global metrics (*Buildings (all types), Population and Utility of Buildings*) following the 2011 February M_w 6.2 Christchurch earthquake. Solid lines indicate GA-optimized results, whereas dashed lines show the mean inferred recovery time.

Nevertheless, as the steep slope of the recovery curve on day 1 and 21 suggests, when critical pipe failures are discovered, the optimization algorithm remains highly efficient. Despite this limitation, taking the lower bound of both the inferred and optimized recovery, the water supply network would have significantly gained in resilience. Equations 13 to 15 quantify the effect of the recovery optimization by looking at the difference of resilience R as described in Equation 3 (ΔR), the resilience loss reduction (ΔLR), and the total absolute gain (G), respectively.

$$\Delta R = R_{Inferred} - R_{Optimized} \tag{13}$$

$$\Delta LR = \frac{\Delta R}{1 - R_{Inferred}} \tag{14}$$

$$G = \Delta R \cdot \text{Quantity}_{Metric} \tag{15}$$

where $R_{Inferred}$ and $R_{Optimized}$ are the resilience of a given metric based on the inferred and optimized recoveries, respectively, and Quantity_{Metric} is the total quantity of a given metric as presented in Subsection 2.1. Table 2 quantitatively presents the benefits of applying the proposed optimization framework.

Table 2. Quantitative summary of the recovery optimization gains for the selected metrics

Metric	Optimized resilience	Resilience gain	Resilience loss reduction	Total absolute gain
	$R_{Optimized}$	ΔR	ΔLR	G
Population	96.4%	0.85%	18.9%	186,000
Utility	94.1%	1.35%	18.5%	186,000
Buildings (all types)	90.4%	2.56%	21.0%	333,000
Business buildings	96.2%	$\ll$0.1%	$\ll$0.1%	288
School buildings	94.8%	1.43%	21.7%	1,980
Medical buildings	99.1%	$\ll$0.1%	$\ll$0.1%	6
Critical buildings	98.9%	0.44%	29.3%	15

It must be noted that results presented in Figures 5 and 6, and in Table 2 only represent the lower-bound improvement possible using the proposed optimization method. By improving the accuracy of the pipe failure prediction, and relaxing the constraints of constant repair and inspection rates, a greater optimization would be possible.

REAL-TIME APPLICATION

As can be derived from the discussion in the previous section, applying this framework on a real-time recovery would necessitate some adjustments on how the inspection priorities are established, the pipe failure database is managed and the repair capacity is estimated.

The proposed inspection method assesses pipeline integrity based on the score it obtained from Equation 4 irrespective of its relative location in respect with other inspections to be carried out. Two problems arise from this. First, inspections are not, and cannot, be carried out this way as inspection teams do not inspect small pipelines individually. Instead, they try to discover pipe failures in one specific area and move to the next one once the network is believed restored at the present location. Hence, the inspection list should be used as an indicator to target areas in which the inspection teams' work will have the highest chances of discovering critical pipe failures. The second problem is the noted poor performance of the individual pipe failure estimation. This can be improved following two different approaches. As already noted, the first option would be the use of improved fragility functions based on more advanced statistical methods. A second option would be to combine post-earthquake LiDAR survey to assess land damage, as it was the case following the major events from the Canterbury Earthquake Sequence (Hughes et al., 2015), with ground strain-based pipeline fragility functions (e.g. O'Rourke et al., 2014; Bouziou and ORourke, 2017). This option would remove the intensity measure uncertainty by direct observations, but is unable to assess damage due to transient ground motion. Further research is needed to explore the potential of such ideas. A third option could consist of a periodic Bayesian update of the pipe probability of failure based on observations obtained during the damage inspections throughout the recovery itself. Subsequently, the inspection priority score can be re-evaluated and inspections would be redirected to more critical locations. Note also that some situations (e.g. major medical facility deprived from water) may require more holistic approaches such that the operator will prioritize inspections in potentially less damage areas in order to remedy critical issues.

During the inspection process, some of the discovered pipe failures might not be critical (i.e. they do not hinder the global functioning of the network). Hence, these failures should not be included into the database used by the genetic algorithm to generate solutions, but left for the post-recovery phase as part of a long-term effort to restore or enhance the network quality.

As the inspection capacity was only useful to infer the recovery, the only constraint of the problem becomes the repair capacity. The availability of this resource significantly fluctuates over time and should therefore be carefully and periodically assessed. Two factors can influence the periodic repair capacity. First, the number of repair teams can vary over time as noted by Eidinger and Tang (2012, pp. 159), and second repairing trunk main and main pipelines generally requires more resources and time than repairing submain pipelines as noted by Federal Emergency Management Agency (2003, Table 8.1.c) and Cousins (2013, Table A.4.3). By constantly re-assessing the repair capacity and updating the pipe failure database, this framework could be applied on a daily basis, helping emergency managers to efficiently implement their strategy.

In some instances, the objective of the emergency manager may differ from that proposed by the algorithm. In such cases, the emergency manager can decide to prioritize the repairs differently than the proposed algorithm. The effective changes in the pipe failure database (executed repairs) will be taken into account in the next assessed repair period. In other words, the algorithm adapts its next solution to the previous manger's decision and not to its own solution.

CONCLUSION

This paper presented an inferred estimation of the Christchurch water supply recovery following the 22 February 2011 M_w 6.2 Christchurch earthquake and subsequently the development of a genetic algorithm method to optimize the recovery of such systems for potential future events. Based on reported network performance and for a network possessing well-distributed water sources, it was shown that a connectivity analysis is sufficient to estimate the disruption once the majority of the pump stations are operational. As noted in other prior studies, the performance of water supply network is therefore strongly correlated with the power availability to pump stations. However, pipe failures remain a critical factor to restore services, with approximately 30% of buildings remaining without water access after electricity was restored to the majority of the city.

The presented optimization method, as applied to this case study, reduced the proportion disruption after two days by approximately 30% and reduced overall system resilience loss by 20%. However, the restoration of the water services would have taken longer in some areas due to the inefficiency of the adopted pipeline fragility function to accurately determine the probability of individual pipe failure. It must also be noted that no optimization was realized on the restoration of facilities (e.g. pump stations or wells). A global optimization on facilities and pipes could be carried out by iteratively combining the proposed model with a facility restoration model (e.g. Xu et al., 2007). Utilizing this framework, further studies can also determine the optimal number of repair teams deploy following an event. The same methodology could also be applied to other lifelines such as the sewerage system, the gas distribution network or the telecommunication network. Finally, it must be stressed that, combining the best of both the human holistic approach of such a problem and the optimized tactical solutions created by the algorithm would significantly reduce the indirect losses due to lifeline disruption.

DATA AND RESOURCES

Matthew Hughes (University of Canterbury) provided the building footprint, land usage, meshblock, liquefaction resistance index and ground motion intensity maps as well as the water supply network and pipe failures databases. The power outage map was developed and provided by Roger Paredes and Leonardo Dueñas-Osorio (Rice University). Census information of each meshblock can be found at: `http://www3.stats.govt.nz/meshblock/2013/excel/2013_mb_dataset_Canterbury_Region.zip?_ga=2.241809418.94925561.1523564544-257358082.1516912122`. The authors developed an object-oriented software in C/C++ utilizing the Intel Math Kernal Library (Intel, 2017a) as well as the Intel Message Passing Interface library (Intel, 2017b) for the computation performed. These packages must be installed in order to compile and execute the program. The source code is available in the github repository: `https://github.com/xavierbellagamba/NetworkRecovery`.

ACKNOWLEDGEMENT

The authors thank the three anonymous peer-reviewers, whose comments help to improve the overall quality of this study as well as Irmana Sampedro Garcia and Karn Snyder-Bishop (Christchurch City Council) for sharing their insights on the historical recovery. Matthew Hughes (University of Canterbury) provided several datasets used in the study as well as some insights on the historical recovery. Roger Paredes and Leonardo Dueñas-Osorio (Rice University) shared their power outage dataset. This project was supported by QuakeCoRE, a New Zealand Tertiary Education Commission-funded Centre, Resilience to Nature's Challenges, a Science National Challenge overseen by the New Zealand Ministry of Business, Innovation and Employment, and also the Royal Society of New Zealand Rutherford Discovery Fellowship. This is QuakeCoRE publication number 0297.

REFERENCES

Bagriacik, A., Davidson, R., Bradley, B., Hughes, M., and Cubrinovski, M., 2018. Comparison of Statistical and Machine Learning Approaches to Modeling Earthquake Damage to Water Pipelines. *Soil Dynamics and Earthquake Engineering* **112**, 76–88.

Bellagamba, X., Bradley, B., Wotherspoon, L., and Hughes, M., Accepted. Development and validation of fragility functions for buried pipelines based on Canterbury earthquake sequence data. *Earthquake Spectra* .

Bocchini, P., Deodatis, G., and Ellingwood, B., 2013. Computational procedure for the assisted multi-phase resilience-oriented disaster management of transportation systems. *G. Deodatis, BR Elling-*

wood, & Frangopol (Eds.), Safety, reliability, risk, and life-cycle performance of structures and infrastructures pp. 581–588.

Borden, F., 1997. *The 1994 Northridge earthquake and the fires that followed*. Building and Fire Research Laboratory, National Institute of Standards and Technology.

Bouziou, D. and ORourke, T., 2017. Response of the Christchurch water distribution system to the 22 February 2011 earthquake. *Soil Dynamics and Earthquake Engineering* **97**, 14–24.

Bouziou, D., ORourke, T., Cubrinovski, M., and Henderson, D., 2015. Evaluation of ground deformations during the 2010–2011 Canterbury earthquake sequence. In *Proceedings of the* 6^{th} *International Conference on Earthquake Geotechnical Engineering*. Christchurch, New Zealand.

Bradley, B., 2014. Site-specific and spatially-distributed ground-motion intensity estimation in the 2010–2011 Canterbury earthquakes. *Soil Dynamics and Earthquake Engineering* **61**, 83–91.

Bradley, B. and Cubrinovski, M., 2011. Near-source strong ground motions observed in the 22 February 2011 Christchurch earthquake. *Seismological Research Letters* **82**, 853–865.

Bradley, B., Quigley, M., Van Dissen, R., and Litchfield, N., 2014. Ground motion and seismic source aspects of the Canterbury earthquake sequence. *Earthquake Spectra* **30**, 1–15.

Bruneau, M., Chang, S., Eguchi, R., Lee, G., O'Rourke, T., Reinhorn, A., Shinozuka, M., Tierney, K., Wallace, W., and von Winterfeldt, D., 2003. A framework to quantitatively assess and enhance the seismic resilience of communities. *Earthquake spectra* **19**, 733–752.

Chang, S., Taylor, J., Elwood, K., Seville, E., Brunsdon, D., and Gartner, M., 2014. Urban disaster recovery in Christchurch: the central business district cordon and other critical decisions. *Earthquake Spectra* **30**, 513–532.

Chen, S., Montgomery, J., and Bolufé-Röhler, A., 2015. Measuring the curse of dimensionality and its effects on particle swarm optimization and differential evolution. *Applied Intelligence* **42**, 514–526.

Choi, C. (ed.), 2017. *Global Prospectus*. The Rockfeller Foundation, New York City, NY.

Chung, R., Ballantyne, D., Comeau, E., Holzer, T., Madrzykowski, D., Schiff, A., Stone, W., Wilcoski, J., Borcherdt, R., Cooper, J. et al., 1996. *January 17, 1995 Hyogoken-Nanbu (Kobe) Earthquake: Performance of Structures, Lifelines, and Fire Protection Systems (NIST SP 901)*. *Tech. rep.*, National Institute of Standards and Technology.

Cimellaro, G., Reinhorn, A., and Bruneau, M., 2010. Framework for analytical quantification of disaster resilience. *Engineering Structures* **32**, 3639–3649.

Cousins, J., 2013. *Wellington Without Water - Impact of Large Earthquakes*. *Tech. rep.*, GNS Science Report, Lower Hutt, New Zealand.

Cubrinovski, M., Bradley, B., Wotherspoon, L., Green, R., Bray, J., Wood, C., Pender, M., Allen, J., Bradshaw, A., Rix, G. et al., 2011. Geotechnical aspects of the 22 February 2011 Christchurch earthquake. *Bulletin of the New Zealand Society for Earthquake Engineering* **44**, 205–226.

Cubrinovski, M., Hughes, M., Bradley, B., Noonan, J., Hopkins, R., McNeill, S., and English, G., 2014. *Performance of horizontal infrastructure in Christchurch city through the 2010-2011 Canterbury earthquake sequence*. *Tech. rep.*, University of Canterbury. Civil and Natural Resources Engineering, Christchurch, New Zealand.

Dahlhamer, J., Tierney, K., and Webb, G., 1999. *Predicting business financial losses in the 1989 Loma Prieta and 1994 Northridge Earthquakes: Implications for loss estimation research*. *Tech. rep.*, Disaster Research Center, University of Delaware, Newark, DE.

Davis, C., 2014. Water system service categories, post-earthquake interaction, and restoration strategies. *Earthquake Spectra* **30**, 1487–1509.

Dellow, G., Yetton, M., Massey, C., Archibald, G., Barrell, D., Bell, D., Bruce, Z., Campbell, A., Davies, T., De Pascale, G. et al., 2011. Landslides caused by the 22 February 2011 Christchurch earthquake and management of landslide risk in the immediate aftermath. *Bulletin of the New Zealand Society for Earthquake Engineering* **44**, 227–238.

Eidinger, J. and Tang, A., 2012. *Christchurch, New Zealand Earthquake Sequence of Mw 7.1 September 04, 2010 Mw 6.3 February 22, 2011 Mw 6.0 June 13, 2011: Lifeline Performance*. *Tech. rep.*, Technical Council on Lifeline Earthquake Engineering, Reston, VA.

Fang, Y. and Sansavini, G., 2017. Emergence of Antifragility by Optimum Postdisruption Restoration Planning of Infrastructure Networks. *Journal of Infrastructure Systems* **23**, 04017024.

Fawcett, T., 2006. An introduction to ROC analysis. *Pattern recognition letters* **27**, 861–874.

Federal Emergency Management Agency, 2003. *HAZUS-MH MR4 Technical Manual*. *Tech. rep.*, National Institute of Building Sciences, Washington DC.

Feng, C.-M. and Wang, T.-C., 2003. Highway emergency rehabilitation scheduling in post-earthquake 72 hours. *Journal of the Eastern Asia Society for Transportation Studies* **5**, 3276–3285.

Fenwick, T., Hoskin, K., and Brunsdon, D., 2011. *Resilience Lessons: Orion's 2010 and 2011 Earthquake Experience*. *Tech. rep.*, Kestrel Group, Wellington, New Zealand.

Fraser, I. (ed.), 2017. *Building Urban Resilience in New Zealand: Lessons from our Major Cities*. Centre for Disaster Resilience, Recovery and Reconstruction, University of Auckland, Auckland, New Zealand.

Giovinazzi, S., Stevenson, J., Mitchell, J., and Mason, A., 2012. Temporary housing issues following the 22nd Christchurch Earthquake, NZ. In *Proceedings of the 2012 New Zealand Society for Earthquake Engineering Conference*, pp. 13–15. New Zealand Society for Earthquake Engineering, Ground Floor, 158 The Terrace Wellington 6144 New Zealand, Christchurch, New Zealand.

Giovinazzi, S., Wilson, T., Davis, C., Bristow, D., Gallagher, M., Schofield, A., Villemure, M., Eidinger, J., and Tang, A., 2011. Lifelines performance and management following the 22 February 2011 Christchurch earthquake, New Zealand: highlights of resilience. *Bulletin of the New Zealand Society for Earthquake Engineering* **44**, 402–417.

Hallegatte, S., 2008. An adaptive regional input-output model and its application to the assessment of the economic cost of Katrina. *Risk analysis* **28**, 779–799.

Haupt, R. and Haupt, S., 1998. *Practical genetic algorithms, second edition*. Wiley Interscience.

Hughes, M., Nayyerloo, M., Bellagamba, X., Morris, J., Brabhaharan, P., Rooney, S., Hobbs, E., Wooley, K., and Hutchison, S., 2017. Impacts of the 14th November 2016 Kaikoura Earthquake on the Three Water Systems in Wellington, Marlborough and Kaikoura, New Zealand: Preliminary Observations. *Bulletin of the New Zealand Society for Earthquake Engineering* **50**, 306–317.

Hughes, M., Quigley, M., van Ballegooy, S., Deam, B., Bradley, B., Hart, D. et al., 2015. The sinking city: Earthquakes increase flood hazard in Christchurch, New Zealand. *GSA Today* **25**.

Hynes, W., Purcell, S., Walsh, S., and Ehimen, E., 2016. *IRGC resource guide on resilience, v29-07-2016*, chap. Formalizing Resilience Concepts for Critical Infrastructure. EPFL International Risk Governance Center (IRGC), Lausanne, Switzerland.

Intel, 2017a. Intel Math Kernel Library.

Intel, 2017b. Intel Message Passing Interface.

Jayaram, N. and Baker, J., 2009. Correlation model for spatially distributed ground-motion intensities. *Earthquake Engineering & Structural Dynamics* **38**, 1687–1708.

King, A., Middleton, D., Brown, C., Johnston, D., and Johal, S., 2014. Insurance: Its role in recovery from the 2010-2011 Canterbury earthquake sequence. *Earthquake Spectra* **30**, 475–491.

Klise, K., Bynum, M., Moriarty, D., and Murray, R., 2017. A software framework for assessing the resilience of drinking water systems to disasters with an example earthquake case study. *Environmental Modelling & Software* **95**, 420–431.

Love, T., 2011. *Population movement after natural disasters: a literature review and assessment of Christchurch data*. *Tech. rep.*, Sapere Research Group, Wellington, New Zealand.

Mallipeddi, R. and Suganthan, P., 2008. Empirical study on the effect of population size on differential evolution algorithm. In *Evolutionary Computation, 2008. CEC 2008.(IEEE World Congress on Computational Intelligence). IEEE Congress on*, pp. 3663–3670. IEEE.

McReynolds, L. and Simmons, R., 1995. LA's rehearsal for the big one. *Journal-American Water Works Association* **87**, 65–70.

Miles, S. and Chang, S., 2006. Modeling community recovery from earthquakes. *Earthquake Spectra* **22**, 439–458.

Mitchell, M., 1998. *An introduction to genetic algorithms*. MIT press.

O'Rourke, T., Jeon, S.-S., Toprak, S., Cubrinovski, M., Hughes, M., van Ballegooy, S., and Bouziou, D., 2014. Earthquake response of underground pipeline networks in Christchurch, NZ. *Earthquake Spectra* **30**, 183–204.

Rose, A., Benavides, J., Chang, S., Szczesniak, P., and Lim, D., 1997. The regional economic impact of an earthquake: Direct and indirect effects of electricity lifeline disruptions. *Journal of Regional Science* **37**, 437–458.

Statistics New Zealand, 2013a. 2013 Census meshblock dataset. http://archive.stats.govt.nz/Census/2013-census/data-tables/meshblock-dataset.aspx.

Statistics New Zealand, 2013b. *The census has been held every five years, with only four exceptions*. http://archive.stats.govt.nz/Census/2013-census/info-about-the-census/intro-to-nz-census/history/did-you-know/every-five-years.aspx[Accessed: May 2018].

Stevenson, J., Becker, J., Cradock-Henry, N., Johal, S., Johnston, D., Orchiston, C., and Seville, E., 2017. Economic and social reconnaissance: Kaikōura Earthquake 2016. *Bulletin of the New Zealand Society for Earthquake Engineering* **50**, 346–355.

Stevenson, J., Kachali, H., Whitman, Z., Seville, E., Vargo, J., and Wilson, T., 2011. Preliminary observations of the impacts the 22 February Christchurch Earthquake had on organisations and the economy: A report from the field (22 February-22 March 2011). *Bulletin of the New Zealand Society for Earthquake Engineering* **44**, 65.

Stevenson, J., Vargo, J., Seville, E., Kachali, H., McNaughton, A., and Powell, F., 2012. *The Recovery of Canterburys Organisations: A comparative analysis of the 4 September 2010, 22 February and 13 June 2011 Earthquake*. *Tech. rep.*, University of Canterbury. Civil and Natural Resources Engineering, Christchurch, New Zealand.

Storn, R., 1996. On the usage of differential evolution for function optimization. In *Fuzzy Information Processing Society, 1996. NAFIPS., 1996 Biennial Conference of the North American*, pp. 519–523. IEEE.

Tabucchi, T., Davidson, R., and Brink, S., 2010. Simulation of post-earthquake water supply system restoration. *Civil Engineering and Environmental Systems* **27**, 263–279.

Tierney, K., 1997. Business impacts of the Northridge earthquake. *Journal of Contingencies and Crisis Management* **5**, 87–97.

Xu, N., Guikema, S., Davidson, R. A., Nozick, L., Çağnan, Z., and Vaziri, K., 2007. Optimizing scheduling of post-earthquake electric power restoration tasks. *Earthquake engineering & structural dynamics* **36**, 265–284.

Yao, M. and Min, K., 1998. Repair-unit location models for power failures. *IEEE Transactions on Engineering Management* **45**, 57–65.

Zorn, C. and Shamseldin, A., 2016. Quantifying directional dependencies from infrastructure restoration data. *Earthquake Spectra* **32**, 1363–1381.

Appendices

ELECTRONIC SUPPLEMENT: PREDICTIVE PERFORMANCE OF THE PIPE DAMAGE AND BUILDING CONNECTIVITY MODEL

This electronic supplement presents the predictive performance details for both the pipe damage and building connectivity analyses. First, the receiver operation characteristics curves are defined and discussed. Second, differences observed between the inferred and predicted metrics are given and interpreted.

Figure A.1 provides a summary of the model performance prediction. Figure A.1 (a) illustrates the cumulative distribution functions (CDF) of the pipes that remained intact (i.e. CDF of the true negatives) and the pipes that failed given the estimated probability of failure of the model (i.e. CDF of the true positives). Figure A.1 (c) exhibits the buildings that remained historically connected to the water supply network (i.e. CDF of the true negatives) and the buildings that were historically disconnected from the water supply network given the estimated probability of disconnection (i.e. CDF of the true positives). Figures A.1(b) and (d) show the receiver operating characteristics (ROC) curve for the pipe failure and building disconnection classification, respectively. The area under these curves (AUC) quantifies the model performance (Fawcett, 2006).

In Figures A.1 (a) and (c), the ideal case (i.e. when the predictions always perfectly match the inferred results) would be vertical CDFs in 0 and 1 for the true negatives and the true positives, respectively. As it can be observed in both Figures A.1(a) and (c), the true negatives are relatively well predicted as the CDFs tends to be relatively steep towards 0 and flatten out as the probability of failure or disconnection increases. However, in Figure A.1 (a), the true positives (observed failed pipes) are poorly predicted. This issue arises from the construction of Poissonian-based fragility functions for horizontal infrastructure, as they are "*less capable of prediction at the individual pipe [...] level*" as noted by Bagriacik et al. (2018). Nevertheless, the global performance remains acceptable with the AUC is equal to 0.7, a value of 1 being perfect. The building disconnection also suffers from a lack of true positive prediction accuracy for several reasons. First, given the high redundancy of the analysed system, the Monte-Carlo simulations of the prediction rarely yields a 100% disconnection probability for a particular building, partially explaining the relatively flat slope below the 95% of disconnection probability. Second, the number of true positives is relatively low compared to the number of the true negatives, inducing less robust results. Nevertheless, the true positive CDF remains below the identity line, indicating a good prediction rate. The goodness of the connection prediction rate is further corroborated by the high AUC (0.92).

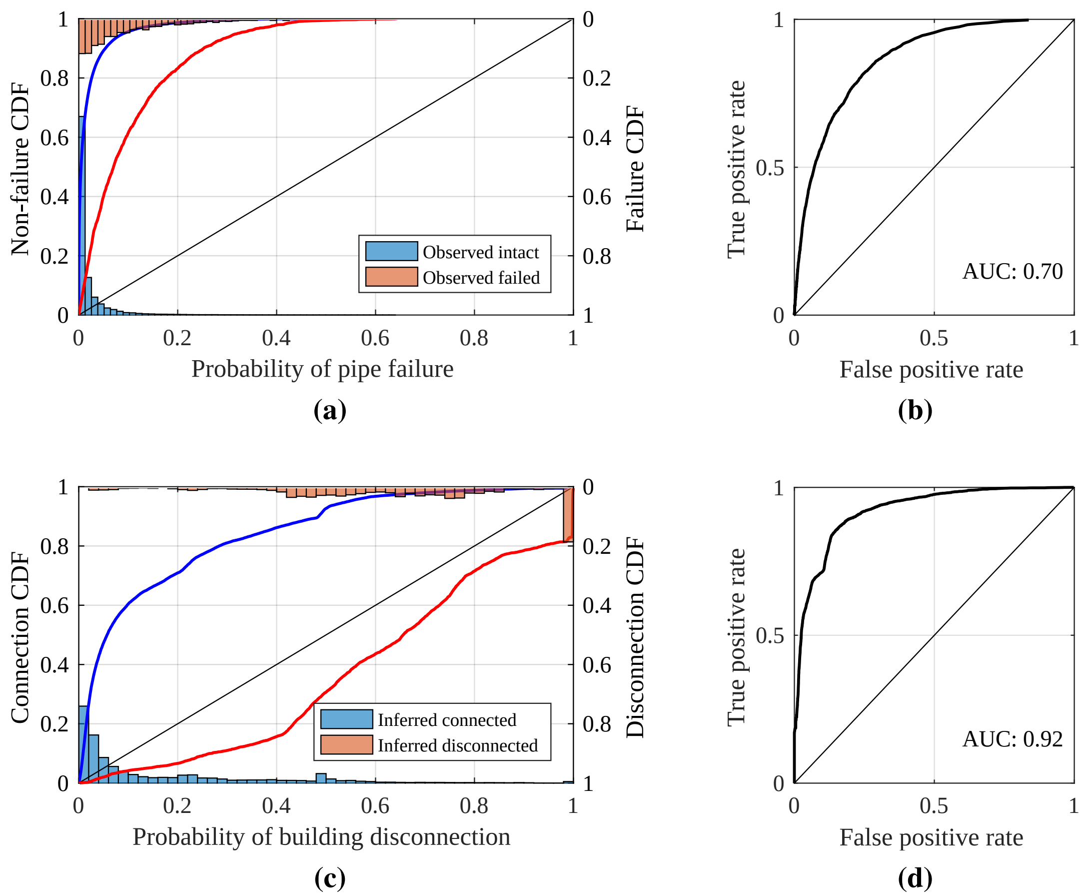

Figure A.1. Performance of the pipe failure modelling as (a) CDFs and histograms of the true negatives (non-failed pipes) in blue and true positives (failed pipes) in red ; and (b) ROC curve ; and performance of the building connection modelling as (c) CDFs and histograms of the true negatives (connected buildings) in blue and true positives (disconnected buildings) in red ; and (d) ROC curve

Figure A.2 compares the values from the co-seismic performance inference of the selected metrics with the prediction distribution. Most of the inferred values remain close to the mode of their respective prediction distribution with the notable exception of the medical buildings. In this case, due to the topology of the network and the location of the buildings, less buildings were deprived of water that what was previously inferred. It is worth noting that there are few medical and critical buildings (377 and 55, respectively) comparatively to the total number of buildings (209,442), leading, in the case of the critical buildings to a non-smooth distribution. The population metric seems to also be slightly overpredicted, whereas the buildings (all types) metric shows the opposite trend. This can indicate that too many residential buildings are predicted to lose their connections to the water supply network and/or that the predicted, impacted areas possess a higher population density than the one simulated from the inferred results. Albeit less pronounced, the same trend can be observed for the utility of buildings.

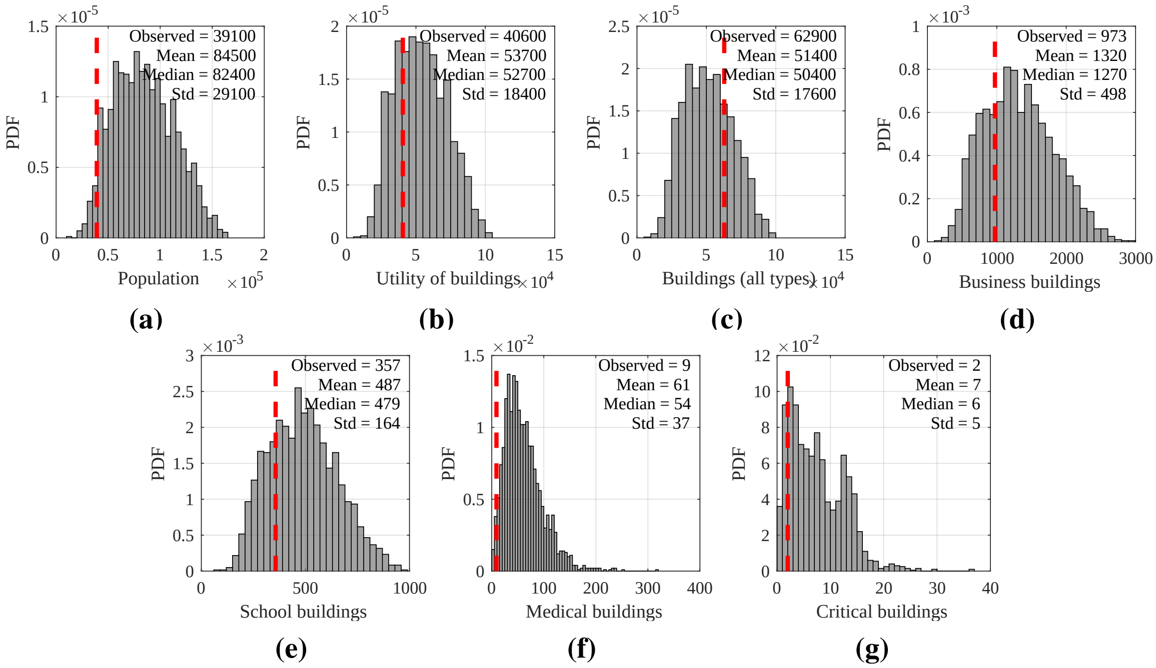

Figure A.2. Histograms of the prediction distribution for the selected metrics showing deprivation of water supply and comparison with inferred actual results (indicated as a red dashed line)